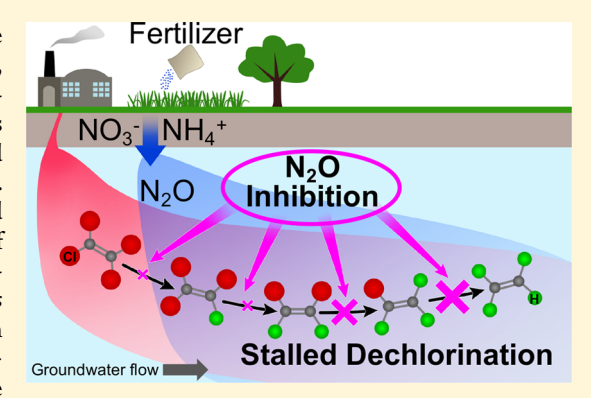


# Nitrous Oxide Is a Potent Inhibitor of Bacterial Reductive Dechlorination

Yongchao Yin,  $^{\dagger, \ddagger, \#}$  Jun Yan,  $^{\dagger, \parallel}$  Gao Chen,  $^{\ddagger, \$}$  Fadime Kara Murdoch,  $^{\dagger, \ddagger, \#}$  Nina Pfisterer,  $^{\dagger, \ddagger, \nabla}$  and Frank E. Löffler  $^{*, \dagger, \ddagger, \$, \perp, \#_{0}}$ 

Supporting Information

**ABSTRACT:** Organohalide-respiring bacteria are key players for the turnover of organohalogens. At sites impacted with chlorinated ethenes, bioremediation promotes reductive dechlorination; however, stoichiometric conversion to environmentally benign ethene is not always achieved. We demonstrate that nitrous oxide  $(N_2O)$ , a compound commonly present in groundwater, inhibits organohalide respiration.  $N_2O$  concentrations in the low micromolar range decreased dechlorination rates and resulted in incomplete dechlorination of tetrachloroethene (PCE) in *Geobacter lovleyi* strain SZ and of *cis-1,2*-dichloroethene (*cDCE*) and vinyl chloride (VC) in *Dehalococcoides mccartyi* strain BAV1 axenic cultures. Presumably,  $N_2O$  interferes with reductive dechlorination by reacting with super-reduced Co(I)—corrinoids of reductive dehalogenases, which is supported by the finding that  $N_2O$  did not inhibit corrinoid-independent fumarate-to-



succinate reduction in strain SZ. Kinetic analyses revealed a best fit to the noncompetitive Michaelis–Menten inhibition model and determined  $N_2O$  inhibitory constants,  $K_{\rm L}$ , for PCE and cDCE dechlorination of 40.8  $\pm$  3.8 and 21.2  $\pm$  3.5  $\mu$ M in strain SZ and strain BAV1, respectively. The lowest  $K_{\rm L}$  value of 9.6  $\pm$  0.4  $\mu$ M was determined for VC to ethene reductive dechlorination in strain BAV1, suggesting that this crucial dechlorination step for achieving detoxification is most susceptible to  $N_2O$  inhibition. Groundwater  $N_2O$  concentrations exceeding 100  $\mu$ M are not uncommon, especially in watersheds impacted by nitrate runoff from agricultural sources. Thus, dissolved  $N_2O$  measurements can inform about cDCE and VC stalls at sites impacted with chlorinated ethenes.

### ■ INTRODUCTION

Chlorinated solvents such as chlorinated ethenes are widespread groundwater contaminants of concern due to their adverse impact on human and ecosystem health.1 The discovery of organohalide-respiring bacteria (OHRB) triggered the development of enhanced bioremediation treatment at sites impacted with chlorinated ethenes. 1,2 Geobacter lovlevi (Geo) strain SZ<sup>3</sup> reductively dechlorinates tetrachloroethene (PCE) via trichloroethene (TCE) to cis-1,2-dichloroethene (cDCE), and several strains of the species Dehalococcoides mccartyi (Dhc)4 and Candidatus Dehalogenimonas etheniformans (Dhgm)<sup>5</sup> reduce cDCE and vinyl chloride (VC) to environmentally benign ethene. Reductive dechlorination is an electron-consuming process, and biostimulation with fermentable substrates to increase the flux of hydrogen is a commonly applied approach to enhance in situ contaminant detoxification.<sup>2,6</sup> Biostimulation alone or combined with bioaugmentation has been applied at many sites impacted with chlorinated ethenes, and substantial

reductions in total organic chlorine are generally achieved; however, declining PCE and TCE concentrations are often associated with increasing trends in *c*DCE and VC concentrations.<sup>7–10</sup> Stalled reductive dechlorination may be due to a lack of electron donor (i.e., hydrogen) or unfavorable geochemical conditions such as the presence of competing electron acceptors (e.g., sulfate), <sup>11,12</sup> the presence of oxygen, <sup>13</sup> low pH conditions, <sup>14</sup> or the absence of organohalide-respiring Dehalococcidia (i.e., *Dhc* and *Dhgm*). <sup>2,18</sup>

Interestingly, a data-mining prediction model applied to geochemical and microbial groundwater monitoring data sets collected from sites impacted with chlorinated ethenes ranked nitrate and nitrite concentrations as the most relevant predictors

Received: October 18, 2018 Revised: December 17, 2018 Accepted: December 18, 2018 Published: December 18, 2018

<sup>†</sup>Department of Microbiology, <sup>‡</sup>Center for Environmental Biotechnology, <sup>§</sup>Department of Civil and Environmental Engineering, and <sup>L</sup>Department of Biosystems Engineering and Soil Science, University of Tennessee, Knoxville, Tennessee 37996, United States

Key Laboratory of Pollution Ecology and Environmental Engineering, Institute of Applied Ecology, Chinese Academy of Sciences, Liaoning 110016, People's Republic of China

Biosciences Division, Oak Ridge National Laboratory, Oak Ridge, Tennessee 37831, United States

for in situ reductive dechlorination and detoxification potential. 16 Microcosm studies have attributed nitrate inhibition of PCE-to-cDCE reductive dechlorination to elevated redox potential;<sup>7,11</sup> however, nitrate had no inhibitory effect on PCE or TCE dechlorination in axenic cultures of Geo strain SZ and Dhc strain FL2.3,17 These contrasting observations can be reconciled if a nitrate transformation product exerts an inhibitory effect on reductive dechlorination. Nitrous oxide (N<sub>2</sub>O) is a known metabolite of microbial nitrogen metabolism including nitrate reduction or ammonium oxidation, 18-21 inhibitory effects of  $N_2O$  on methanogenesis,  $^{22-24}$  and in one case on PCE reductive dechlorination, 11 have been reported. Although detailed mechanistic studies are lacking, a likely explanation is the reaction of N<sub>2</sub>O with cob(I)amides <sup>25,26</sup> and the ensuing inhibition of corrinoid-dependent enzyme systems involved in e.g., methanogenesis.<sup>27</sup> The reductive dehalogenase (RDase) enzyme systems catalyzing carbon-chlorine bond cleavage require a cobamide prosthetic group for function; <sup>28–30</sup> however, the effects of N<sub>2</sub>O on reductive dechlorination by OHRB are largely unclear.

As global fertilizer usage continues to increase and elevated concentrations  $N_2O$  occur in groundwater,  $^{31}$  detailed understanding of the impact of  $N_2O$  on relevant microbial processes, including organohalide respiration, is needed. This study explored the impact of  $N_2O$  on microbial reductive dechlorination and determined inhibitory constants ( $K_I$  values) of  $N_2O$  on reductive dechlorination of PCE in Geo strain SZ and of cDCE and VC in Dhc strain BAV1.

#### ■ MATERIALS AND METHODS

**Chemicals.** PCE, cDCE (both  $\geq$ 99.5%), VC ( $\geq$ 99.5%), ethene ( $\geq$ 99.9%), Vitamin B<sub>12</sub> ( $\geq$ 98%), sodium fumarate ( $\geq$ 98%), and N<sub>2</sub>O ( $\geq$ 99%) were purchased from Sigma-Aldrich (St Louis, MO, USA). All other chemicals used in this study were reagent grade or of higher purity.

**Bacterial Strains and Growth Conditions.** The impact of N<sub>2</sub>O on reductive dechlorination was investigated using two organohalide-respiring isolates: Geo strain SZ, a corrinoidprototroph capable of dechlorinating PCE and TCE to cDCE, 3,32 and Dhc strain BAV1, a corrinoid-auxotroph capable of dechlorinating cDCE and VC to nontoxic ethene. 4,33 Both cultures were grown in 160 mL serum bottles containing a  $CO_{2}$ N<sub>2</sub> (20/80, vol/vol) headspace and 100 mL of synthetic, bicarbonate-buffered (30 mM, pH 7.3) and reduced (0.2 mM Na<sub>2</sub>S and 0.2 mM L-cysteine) mineral salt medium as described. 30,34 Strain SZ cultures received 5 mM acetate as electron donor, 0.28 mM PCE (38 µmol/bottle), 10 mM fumarate, or both PCE and fumarate as electron acceptors, and a vitamin B<sub>12</sub>-free Wolin vitamin solution.<sup>35</sup> Dhc strain BAV1 culture vessels received 10 mL of hydrogen, 0.8 mM (90  $\mu$ mol/ bottle) cDCE or 0.25 mM (40 µmol/bottle) VC, and 5 mM acetate as electron donor, electron acceptor, and carbon source, respectively. Dhc strain BAV1 culture vessels received the Wolin vitamin stock solution containing vitamin B<sub>12</sub> to achieve a final concentration of 25  $\mu$ g L<sup>-1</sup>. For inoculation, culture vessels received 3% (v/v) inocula from actively dechlorinating cultures maintained under the same conditions. All experiments used triplicate culture vessels, and culture bottles without N2O and without inoculum served as positive and negative controls, respectively. Culture vessels were incubated without agitation at 30 °C in the dark with the stoppers facing up.

**Inhibition Experiments.** For *Geo* strain SZ cultures, undiluted N<sub>2</sub>O gas was directly added to incubation vessels

using plastic syringes (BD, Franklin Lakes, NJ, USA) to achieve final aqueous  $N_2O$  concentrations of 9.5, 19.1, and 57.3  $\mu M$  in PCE-amended cultures, of 191.4 µM and 10 mM in fumarateamended cultures, and of 191.4  $\mu$ M in cultures grown with both PCE and fumarate. For Dhc strain BAV1 cultures, undiluted or 10-fold-diluted (with N<sub>2</sub>) N<sub>2</sub>O gas was added with plastic syringes to achieve final aqueous phase N2O concentrations of 9.5, 19.1, and 57.3 µM in cDCE-amended vessels and of 2.9, 5.7, and 19.1 µM in VC-amended vessels. The aqueous phase concentrations (in µM) of N2O in all medium bottles were calculated from the headspace concentrations using a dimensionless Henry's constant of 1.94 for N<sub>2</sub>O at 30 °C<sup>36</sup> according to  $C_{\rm aq} = C_{\rm g}/H_{\rm cc}$ , where  $C_{\rm aq}$ ,  $C_{\rm g}$ , and  $H_{\rm cc}$  are the aqueous concentration (in  $\mu$ M), the headspace concentration (in  $\mu$ mol L<sup>-1</sup>), and the dimensionless Henry's constant, respectively. Average dechlorination rates were calculated based on the continuous accumulation of dechlorination products (i.e., before stable product concentrations were observed). Since each reductive dechlorination step is associated with the release of one chloride ion (Cl<sup>-</sup>), the average dechlorination rates determined in growth experiments are reported as the total amount of Cl<sup>-</sup> released per volume per unit time (i.e.,  $\mu$ mol Cl<sup>-</sup> L<sup>-1</sup> d<sup>-1</sup>).

Whole Cell Suspension Dechlorination Assays. Biomass for whole cell suspension assays was harvested by centrifugation at 10 000g at 4 °C for 30 min from 1.6 L Geo strain SZ and Dhc strain BAV1 cultures that had dechlorinated three feedings of PCE and cDCE, respectively. Inside an anoxic chamber (Coy Laboratory Products Inc., MI, USA), the supernatants were decanted, and the pellets were suspended in 8-10 mL of reduced mineral salts medium. For protein quantification, triplicate 0.2 (strain SZ) and 1.0 mL (strain BAV1) of concentrated cell suspensions were transferred to 2 mL screw cap tubes containing 20 mg of 0.1 mm diameter glass beads, and cells were broken at room temperature using a Bead Ruptor (OMNI, GA, USA) at a speed of 6.0 m s<sup>-1</sup> for three 10 min cycles with 2 min breaks. After centrifugation at 13 000g for 2 min to remove cell debris, protein content in the supernatants was estimated using the Bradford assay<sup>37</sup> on a plate reader (BioTek Instruments, VT, USA). To ensure consistency between replicate experiments, cell suspensions of both isolates were freshly prepared following identical procedures.

Dechlorination assays for rate determinations were performed in 8 mL glass vials sealed with Teflon-lined butyl rubber septa held in place with aluminum crimps. Each vial contained 3.80-4.86 mL of reduced mineral salts medium with 5 mM acetate, a N<sub>2</sub>/CO<sub>2</sub> (80/20, vol/vol) headspace for Geo strain SZ, and a H<sub>2</sub>/CO<sub>2</sub> (80/20, vol/vol) headspace for *Dhc* strain BAV1. Electron donor was provided in at least 40-fold excess of the theoretical demand to ensure that reductive dechlorination was not electron-donor limited. For Geo strain SZ cell suspensions,  $36-1100 \,\mu\text{L}$  of an aqueous 1 mM PCE stock solution was added directly to the assay vials to achieve final aqueous PCE concentrations ranging from 5 to 150 µM. For Dhc strain BAV1 cell suspensions, 2-550  $\mu$ L of cDCE stock (from a 5.0 mM aqueous stock solution) or  $12-630 \mu L$  of VC stock (from a 2.0 mM aqueous stock solution) was added to achieve final aqueous cDCE and VC concentrations ranging from 1 to 500  $\mu$ M and 3 to 150  $\mu$ M, respectively. The total aqueous volume in all vials was 4.9 mL before introducing 0.1 mL of cell suspension. Replicate vials at each initial PCE and cDCE concentration received  $N_2O$  to achieve 0, 10, and 60  $\mu$ M, and VC-amended vials received  $N_2O$  to achieve 0, 15, and 50  $\mu M$  dissolved phase **Environmental Science & Technology** 

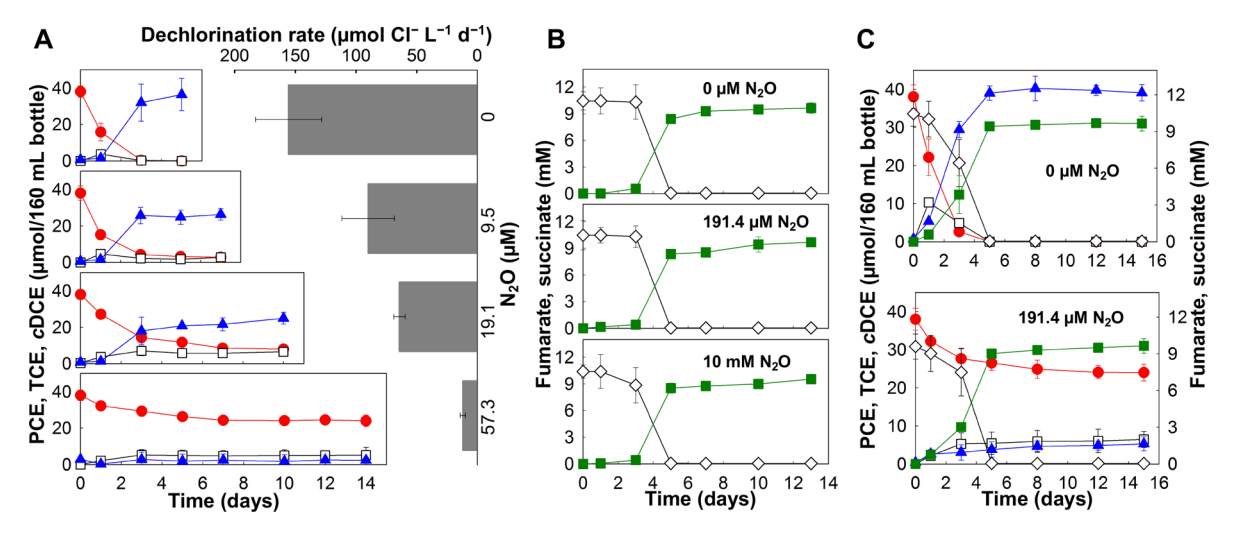


Figure 1. Effect of  $N_2O$  on the consumption of PCE (A), fumarate (B), or both PCE and fumarate (C) as electron acceptors in cultures of the corrinoid–prototrophic bacterium Geo strain SZ. (A) PCE-to-cDCE reductive dechlorination rates and extents in Geo strain SZ cultures without  $N_2O$  (top) and in the presence of 9.5, 19.1, and 57.3  $\mu$ M  $N_2O$ . (B) Fumarate-to-succinate reduction in Geo strain SZ cultures without  $N_2O$  and in the presence of 191.4  $\mu$ M and 10 mM  $N_2O$ . (C) PCE-to-cDCE reductive dechlorination and fumarate-to-succinate reduction in Geo strain SZ cultures in the absence of  $N_2O$  (top) and in the presence of 191.4  $\mu$ M  $N_2O$  (bottom). Solid red circles, PCE; open squares, TCE; solid blue triangles, cDCE; open diamonds, fumarate; solid green squares, succinate. Error bars represent the standard deviation (sd) of triplicate cultures.

N<sub>2</sub>O concentrations. The added N<sub>2</sub>O concentrations were quantified in all assay vials prior to and at the end of the incubation period and determined constant N2O concentrations. Following equilibration, each assay vial received 0.1 mL of the respective cell suspension (corresponding to  $56.3 \pm 2.2 \,\mu g$  of protein per vial for Geo strain SZ and 19.7  $\pm$  1.4  $\mu$ g of protein per vial for Dhc strain BAV1) using plastic syringes to start dechlorination activity. Vials that received 0.1 mL of sterile mineral salt medium instead of cell suspension and vials that received 0.1 mL of heat-killed cell suspension served as negative controls. During the 6 h assay incubation, liquid samples (1 mL) were collected from sacrificial assay vials every 60 min and transferred to 20 mL glass autosampler vials containing 0.1 mL of 25 mM H<sub>2</sub>SO<sub>4</sub> to terminate dechlorination activity. The cell titers and substrate concentrations were chosen such that the dechlorination rates could be determined within the 6 h incubation period and no more than 80% of the initial chlorinated ethene concentration had been consumed at the end of the incubation period.

Analytical Procedures. Chlorinated ethenes and ethene were analyzed with an Agilent G1888 headspace sampler connected to an Agilent 7890 gas chromatograph (GC) equipped with a flame ionization detector (method detection limit  $\approx 0.2 \,\mu\text{M}$ ) and a DB-624 capillary column (60 m length  $\times$ 0.32 mm diameter, 1.8  $\mu$ m film thickness).<sup>34</sup> Fumarate and succinate were quantified using an Agilent 1200 series highperformance liquid chromatography system equipped with an Aminex HPX-87H column and a dual-wavelength absorbance detector set to 210 nm.  $^{38}$  N<sub>2</sub>O was analyzed by injecting 100  $\mu$ L headspace samples into an Agilent 7890A GC equipped with an HP-PLOT Q column (30 m length × 0.320 mm diameter, 20  $\mu$ m film thickness) and a microelectron capture detector. The OD measurements were conducted with a PerkinElmer Lambda 35 UV-vis spectrophotometer by transferring 1 mL cell suspension into a cuvette and recording readings at 600 nm.

**Dechlorination Kinetics and Inhibition Models.** The shortest doubling times reported for *Geo* strain SZ and *Dhc* strain BAV1 are 6 h<sup>3</sup> and 2.2 days, 4,33 respectively. Therefore, additional cell growth was considered negligible over the assay

period (<6 h) and confirmed by constant OD<sub>600</sub> values. For this reason, the Michaelis-Menten model (Table S1), rather than the Monod model for systems involving cell growth, was used to analyze the cell suspension dechlorination data. Therefore, the half-velocity constant  $K_m$ , rather than the Monod half-saturation constant  $K_s$ , was applied in the analyses of cell suspension kinetic parameters. For each treatment at a different initial substrate concentration [S], an initial dechlorination rate v, normalized to the amount of protein per vial, in units of nmol Cl- released min<sup>-1</sup> mg protein<sup>-1</sup>, was calculated from the sum of all dechlorination products measured with the GC. In brief, the amended PCE, cDCE, or VC concentrations in the respective assay vials served as the initial substrate concentrations, and the corresponding dechlorination rates were determined from the slope of progression curves representing total Cl<sup>-</sup> released. The linear regression analysis included five data points and at least three for the assays with a low initial chlorinated ethene concentration. Thus, each datum point in the Michaelis-Menten plots represents a dechlorination rate extracted from one initial substrate concentration (Tables S2-S4).

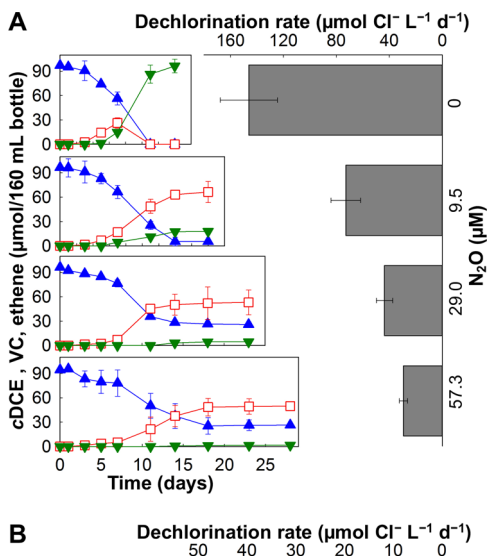
The maximum dechlorination rate  $V_{\mathrm{max}}$  and the half-velocity constant  $K_{\rm m}$  for each treatment were calculated using the Michaelis-Menten nonlinear regression method in the Enzyme Kinetics Module for SigmaPlot 13 (Systat Software Inc., Chicago, IL, USA). This software module evaluated competitive, noncompetitive, and uncompetitive inhibition models for best fit to the rate data based on the highest coefficient of determination  $(R^2)$ , the lowest corrected Akaike's Information Criterion (AICc) values, and the lowest standard deviation of the residuals (Sy.x.). The best-fit model (i.e., noncompetitive inhibition) was used to determine the inhibitory constant,  $K_{I}$ , for N<sub>2</sub>O on reductive dechlorination. For data visualization, Michaelis-Menten (V over [S]), Lineweaver-Burk (1/V over 1/[S]), and Dixon (1/V over [I]) plots were generated using the SigmaPlot Enzyme Kinetics Module for each inhibition model and the different electron acceptors (i.e., PCE, cDCE, and VC).

#### RESULTS

N<sub>2</sub>O Affects Reductive Dechlorination Performance in Geobacter lovleyi Strain SZ Cultures. In the absence of N<sub>2</sub>O, *Geo* strain SZ cultures completely dechlorinated  $38.1 \pm 3.1 \,\mu$ mol of PCE to stoichiometric amounts of cDCE over a 5 day incubation period, and an average PCE-to-cDCE dechlorination rate of 155.6  $\pm$  27.2  $\mu$ mol Cl<sup>-</sup>L<sup>-1</sup> d<sup>-1</sup> was measured (Figure 1A). Cultures amended with 9.5  $\mu$ M or higher concentrations of N<sub>2</sub>O exhibited decreased dechlorination rates and incomplete PCE-to-cDCE dechlorination. In the presence of 9.5 uM N<sub>2</sub>O. Geo strain SZ cultures dechlorinated the initial amount of PCE  $(38.0 \pm 3.9 \ \mu \text{mol})$  at a rate of  $90.0 \pm 21.6 \ \mu \text{mol Cl}^- \ \text{L}^{-1} \ \text{d}^{-1}$ , leading to an extended time period of at least 7 days to achieve complete consumption of PCE. Although PCE was completely consumed in cultures that received 9.5 µM N<sub>2</sub>O, small amounts of TCE (7.6  $\pm$  0.3  $\mu$ mol) remained, even after an extended incubation period of 180 days (data not shown). With the addition of 19.1 µM N<sub>2</sub>O, the average PCE dechlorination rate in Geo strain SZ cultures decreased to  $64.2 \pm 4.6 \ \mu mol \ Cl^- \ L^{-1}$  $d^{-1}$ , and no more than 78  $\pm$  3.4% of the initial amount of PCE  $(38.5 \pm 1.1 \, \mu \text{mol})$  was dechlorinated. Following an extended incubation period of 180 days, PCE (9.9  $\pm$  0.2  $\mu$ mol), TCE (6.6  $\pm$  1.6  $\mu$ mol), and cDCE (25.0  $\pm$  3.2  $\mu$ mol) were measured in strain SZ cultures that had received an initial dose of  $38.5 \pm 1.1$  $\mu$ mol of PCE and 19.1  $\mu$ M N<sub>2</sub>O. A further decline in dechlorination rate to 12.0  $\pm$  2.1  $\mu$ mol Cl<sup>-</sup> L<sup>-1</sup> d<sup>-1</sup> was observed in cultures that received 57.3  $\mu$ M N<sub>2</sub>O, and 63.4  $\pm$ 4.5% of the initial amount of PCE (38.3  $\pm$  3.7  $\mu$ mol) remained in culture bottles at the termination of the experiments (Figure 1A). In all culture bottles with observed inhibition of dechlorination activity, electron donor (i.e., 5 mM acetate) was not limiting electron-acceptor reduction. Furthermore, consistent with the absence of N2O reductase (nos) operons in the genome of Geo strain SZ, 32 the amended N<sub>2</sub>O remained constant throughout the experiment.

In addition to catalyzing PCE-to-cDCE dechlorination, Geo strain SZ also derives energy from acetate oxidation coupled to fumarate to succinate reduction.<sup>3</sup> In contrast to organohalide respiration catalyzed by corrinoid-dependent reductive dehalogenases, fumarate respiration via fumarate reductase does not involve a corrinoid-dependent enzyme system.<sup>39</sup> Therefore, investigating the impact of N2O on fumarate reduction by Geo strain SZ cultures served as a control experiment to illustrate the selective effect of N<sub>2</sub>O on the PCE RDase in Geo strain SZ. As shown in Figure 1B, the presence of 191.4  $\mu$ M and 10 mM N<sub>2</sub>O did not impact fumarate to succinate reduction rates and extents in Geo strain SZ cultures. In the absence of N2O, Geo strain SZ reduced PCE and fumarate concomitantly (Figure 1C, top); however, in cultures amended with 191.4 µM N2O, only fumarate was reduced to succinate and no PCE reductive dechlorination occurred (Figure 1C, bottom).

N<sub>2</sub>O Affects cDCE and VC Reductive Dechlorination Performance in *Dhc* strain BAV1 Cultures. Without N<sub>2</sub>O, *Dhc* strain BAV1 dechlorinated cDCE (97.2  $\pm$  3.1  $\mu$ mol) to stoichiometric amounts of ethene (102.3  $\pm$  6.1  $\mu$ mol) within a 14-day incubation period at an average cDCE-to-ethene dechlorination rate of 146.1  $\pm$  21.6  $\mu$ mol Cl<sup>-</sup> L<sup>-1</sup> d<sup>-1</sup> (Figure 2A). In contrast, cultures amended with 9.5  $\mu$ M or higher N<sub>2</sub>O concentrations all exhibited incomplete transformation of cDCE and VC and required longer incubation periods (up to 28 days) before stable dechlorination product patterns were observed. Cultures that received 9.5  $\mu$ M N<sub>2</sub>O showed a significantly lower



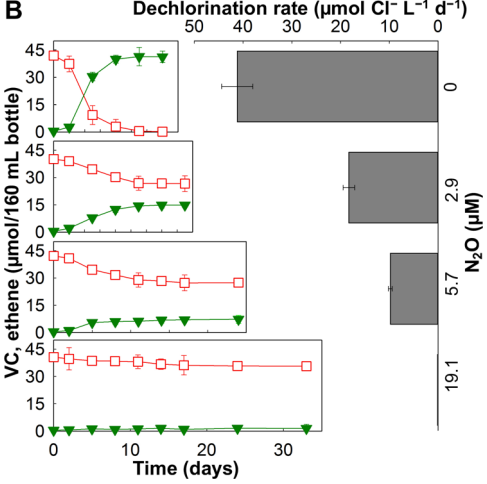


**Figure 2.** Effect of N<sub>2</sub>O on reductive dechlorination of *c*DCE (A) and VC (B) in corrinoid auxotrophic *Dhc* strain BAV1. (A) *c*DCE reductive dechlorination rates and extents in *Dhc* strain BAV1 without N<sub>2</sub>O (top panel) and in the presence of 9.5, 29.0, and 57.3  $\mu$ M N<sub>2</sub>O. (B) VC reductive dechlorination rates and extents in *Dhc* strain BAV1 without N<sub>2</sub>O (top) and in the presence of 2.9, 5.7, and 19.1  $\mu$ M N<sub>2</sub>O. Solid blue triangles, *c*DCE; open red squares, VC; inverted, solid green triangles, ethene. Error bars represent the sd of triplicate cultures.

dechlorination rate of 66.8  $\pm$  21.6  $\mu$ mol Cl<sup>-</sup> L<sup>-1</sup> d<sup>-1</sup>, and the initial amount of cDCE (97.2  $\pm$  1.2  $\mu$ mol) was dechlorinated to a mixture of VC (74.1  $\pm$  1.2  $\mu$ mol) and ethene (23.1  $\pm$  0.7 μmol). Cultures that received 29.0 μM N<sub>2</sub>O dechlorinated only about one-half (50.7  $\pm$  3.3%) of the initial amount of cDCE  $(96.3 \pm 1.1 \,\mu\text{mol})$  to predominantly VC  $(48.8 \pm 3.2 \,\mu\text{mol})$  at a rate of 24.4  $\pm$  1.1  $\mu$ mol Cl<sup>-</sup> L<sup>-1</sup> d<sup>-1</sup>, and only small amounts of ethene (4.7  $\pm$  0.2%) were produced. At a higher N<sub>2</sub>O concentration of 57.3 µM, strain BAV1 dechlorinated cDCE to VC at a dechlorination rate of 18.9  $\pm$  0.7  $\mu$ mol Cl<sup>-</sup> L<sup>-1</sup> d<sup>-1</sup>, no ethene was formed, and about one-third (26.3  $\pm$  0.4  $\mu$ mol) of the initial amount of cDCE remained. Extended incubation periods of up to 6 months did not result in further dechlorination in all tested strain BAV1 culture vessels with N<sub>2</sub>O. Notably, in all N<sub>2</sub>O-amended Dhc strain BAV1 cultures, the VC-to-ethene dechlorination step occurred at such low rates resulting in VC rather than ethene formation as the major product.

To further investigate the impact of  $N_2O$  on the reductive dechlorination of VC, *Dhc* strain BAV1 cultures amended with VC as electron acceptor received  $N_2O$  at concentrations of 2.9,

5.7, and 19.1  $\mu$ M. Cultures without N<sub>2</sub>O completely dechlorinated the initial amount of 41.2  $\pm$  0.4  $\mu$ mol of VC to ethene within 11 days at an average VC dechlorination rate of  $37.2 \pm 2.7 \mu \text{mol Cl}^{-1} \text{ L}^{-1} \text{ d}^{-1}$  (Figure 2B). N<sub>2</sub>O had a profound impact on VC dechlorination in Dhc strain BAV1 cultures, and the VC dechlorination rates decreased to 18.3  $\pm$  2.1 and 9.8  $\pm$ 0.4  $\mu$ mol Cl<sup>-</sup> L<sup>-1</sup> d<sup>-1</sup> in the presence of 2.9 and 5.7  $\mu$ M N<sub>2</sub>O<sub>3</sub> respectively. Compared to the complete VC to ethene conversion in control incubations without N<sub>2</sub>O, the amount of VC dechlorinated to ethene was diminished by  $37.0 \pm 1.3\%$  and  $76.2 \pm 4.1\%$ , respectively, in cultures amended with 2.9 and 5.7  $\mu$ M N<sub>2</sub>O. The most pronounced inhibition was observed in *Dhc* strain BAV1 cultures that received 19.1  $\mu$ M of N<sub>2</sub>O (Figure 2B), and only negligible amounts (<1.6  $\pm$  0.6  $\mu$ mol) of ethene were formed even after extended incubation periods of 180 days, indicating that the VC to ethene step was particularly susceptible to N<sub>2</sub>O inhibition.

Quantification of N2O Inhibition in Whole Cell Suspension Dechlorination Assays. To further investigate the inhibitory effects of N<sub>2</sub>O on reductive dechlorination, whole cell suspension assays were performed. Plots of dechlorination rates versus initial substrate concentrations with increasing N<sub>2</sub>O concentrations are presented in Figures 3 and 4. In all cases, the maximum dechlorination rates decreased with the addition of increasing N2O concentrations. In Geo strain SZ cell suspensions

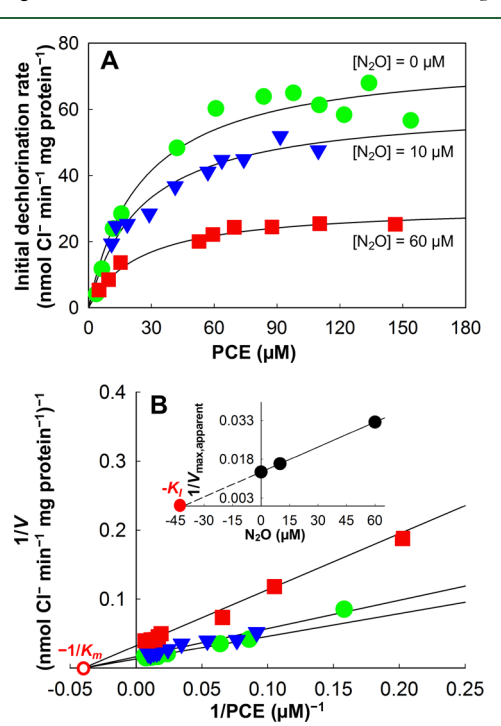


Figure 3. Kinetics of PCE-to-cDCE reductive dechlorination in cell suspensions of Geo strain SZ in the presence of increasing concentrations of N2O. (A) Michaelis-Menten plot of initial PCEto-cDCE dechlorination rates versus PCE concentrations without and in the presence of 10 and 60  $\mu$ M N<sub>2</sub>O. (B) Lineweaver–Burk plot with inserted Dixon plot illustrating N2O inhibition on PCE-to-cDCE reductive dechlorination. Solid lines represent the best fit to each data set based on nonlinear regression using the noncompetitive inhibition model. Solid green circles represent rate data measured in the absence of N2O, solid blue triangles show rate data measured in the presence of 10  $\mu$ M N<sub>2</sub>O, and solid red squares show rate data measured in the presence of  $60 \, \mu \text{M N}_2\text{O}$ . Solid and open red circles depict the graphical determination of  $-K_{\rm I}$  and  $-1/K_{\rm m}$ , respectively.

without N2O addition, a maximum PCE-to-cDCE dechlorination rate  $(V_{\text{max,PCE}})$  of 76.3  $\pm$  2.6 nmol Cl<sup>-</sup> released min<sup>-1</sup> mg protein<sup>-1</sup> was calculated using nonlinear regression in the Michaelis-Menten model (Figure 3A and Table 1). With the addition of 10 and 60  $\mu$ M N<sub>2</sub>O,  $V_{\rm max,PCE}$  in Geo strain SZ cell suspensions declined to 61.3  $\pm$  4.1 and 30.9  $\pm$  4.2 nmol Cl<sup>-</sup> released min<sup>-1</sup> mg protein<sup>-1</sup>, respectively. Even more pronounced inhibitory effects of N<sub>2</sub>O were observed for cDCE and VC dechlorination in Dhc strain BAV1 assays. In the presence of 10 and 60 µM N<sub>2</sub>O, the maximum cDCE-to-VC dechlorination rate decreased from a  $V_{\text{max,cDCE}}$  of 119.4  $\pm$  2.1 nmol Cl<sup>-</sup> released min<sup>-1</sup> mg protein<sup>-1</sup> in assays without N<sub>2</sub>O to  $81.1 \pm 5.1$  and  $31.2 \pm 2.4$  nmol Cl<sup>-</sup> released min<sup>-1</sup> mg protein<sup>-1</sup>, respectively (Figure 4A and Table 1). The strongest inhibitory effect of N2O was observed in whole cell suspension assays of strain BAV1 with VC as electron acceptor. Compared to the maximum VC-to-ethene dechlorination rate  $V_{\text{max,VC}}$  of 123.3  $\pm$ 2.2 nmol Cl<sup>-</sup> released min<sup>-1</sup> mg protein<sup>-1</sup> without N<sub>2</sub>O, the addition of 15 and 50  $\mu$ M N<sub>2</sub>O reduced  $V_{\rm max,VC}$  to 78.9  $\pm$  2.1 and  $19.9 \pm 1.3 \text{ nmol Cl}^{-1} \text{ released min}^{-1} \text{ mg protein}^{-1}$ , respectively (Figure 4C and Table 1). No dechlorination was detected in control incubations (data not shown), confirming that suspended cells, rather than any abiotic reactions, were responsible for the observed dechlorination activity.

Kinetic Parameters Reveal Pronounced N2O Inhibition. The experimental data generated in Geo strain SZ cell suspension assays (Table S2) fit the Michaelis-Menten model and the corresponding Lineweaver-Burk plot  $(R^2 > 0.95)$ (Figure 3, Figure S1). A maximum PCE dechlorination rate  $V_{\text{max,PCE}}$  of  $76.3 \pm 2.6$  nmol Cl<sup>-</sup> released min<sup>-1</sup> mg protein<sup>-1</sup> and a half-velocity constant  $K_{\text{m,PCE}}$  of 25.1  $\pm$  2.9  $\mu\text{M}$  characterized PCE-to-cDCE dechlorination kinetics for strain SZ in the absence of N<sub>2</sub>O (Table 1, Figure 3B). Without N<sub>2</sub>O and in the presence of 10 and 60 µM N2O, the PCE-to-cDCE dechlorination data fit the competitive, uncompetitive, and noncompetitive inhibition models ( $R^2 > 0.90$ ); however, the noncompetitive inhibition model exhibited the highest  $R^2$  and the lowest AICc and Sy.x. values (Figure 3 and Table S5). Using the noncompetitive inhibition model, an inhibitory constant,  $K_{\rm I}$ , of N<sub>2</sub>O for PCE dechlorination in Geo strain SZ whole cell suspensions of 40.8  $\pm$  3.8  $\mu$ M was determined (inserted Dixon plot, Figure 3B; Table 1).

The experimental data generated in Dhc strain BAV1 whole cell suspension assays (Tables S3 and S4) also fit the Michaelis-Menten model simulations and the corresponding Lineweaver— Burk plots ( $R^2 > 0.90$ ) (Figure 4, Figures S2 and S3). In the presence of increasing N<sub>2</sub>O concentrations, both cDCE-to-VC and VC-to-ethene reductive dechlorination data showed the best fit to the noncompetitive inhibition model based on the highest R<sup>2</sup> and the lowest AICc and Sy.x. values (Figure 4 and Table S5). While *Dhc* strain BAV1 assays produced comparable  $V_{
m max,cDCE}$  and  $V_{
m max,VC}$  values of 119.4  $\pm$  2.1 and 123.3  $\pm$  2.2 nmol Cl $^-$  released min $^{-1}$  mg protein $^{-1}$ , respectively, the  $K_{
m I}$  of  $N_{
m 2}$ O for cDCE dechlorination (21.2  $\pm$  3.5  $\mu$ M) was approximately 2-fold greater than that for VC dechlorination (9.6  $\pm$  0.4  $\mu$ M) (inserted Dixon plots, Figures 4B and 4D; Table 1), consistent with the greater inhibitory effect of N2O observed for the VC dechlorination step. To investigate if the differences in susceptibility of the cDCE and VC dechlorination steps to N2O resulted from different affinities of the BvcA RDase for cDCE and VC, the  $K_{\rm m}$  values for these two electron acceptors were compared. On the basis of the Dhc strain BAV1 assays, similar  $K_{\text{m,cDCE}}$  (19.9  $\pm$  2.5  $\mu$ M) and  $K_{\text{m,VC}}$  (18.9  $\pm$  1.3  $\mu$ M)

**Environmental Science & Technology** 

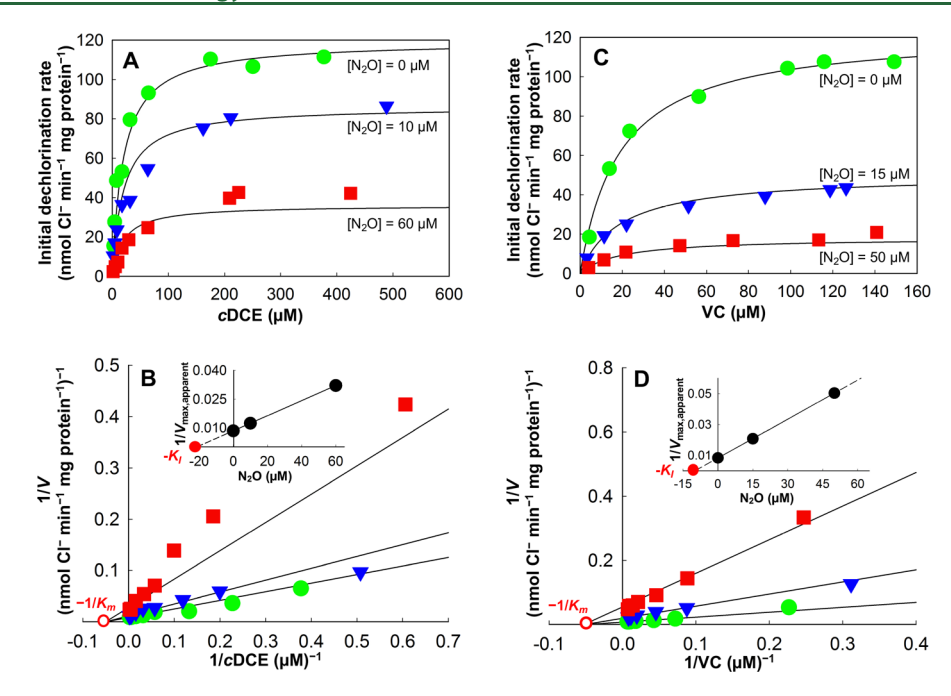


Figure 4. Kinetics of cDCE-to-VC and VC-to-ethene reductive dechlorination in cell suspensions of Dhc strain BAV1 in the presence of increasing concentrations of  $N_2O$ . (A) Michaelis—Menten plot of initial cDCE-to-VC dechlorination in cell suspensions of Dhc strain BAV1 without and in the presence of 10 and 60  $\mu$ M  $N_2O$ . (B) Lineweaver—Burk plot with inserted Dixon plot illustrating  $N_2O$  inhibition of cDCE-to-VC reductive dechlorination. (C) Michaelis—Menten plot of initial VC-to-ethene dechlorination in cell suspensions of Dhc strain BAV1 without and in the presence of 15 and 50  $\mu$ M  $N_2O$ . (D) Lineweaver—Burk plot with inserted Dixon plot illustrating  $N_2O$  inhibition of VC-to-ethene reductive dechlorination. Solid lines represent the best fit to each data set based on nonlinear regression using the noncompetitive inhibition model. Solid green circles represent rate data measured in the absence of  $N_2O$ ; solid blue triangles and solid red squares show dechlorination rate data measured in the presence of  $N_2O$  (panels A and B, cDCE; panels C and D, VC). Solid and open red circles shown in B and D depict the graphical determination of  $-K_1$  and  $-1/K_{mv}$  respectively.

Table 1. Kinetic  $(V_{\text{max}}, K_{\text{m}})$  and Inhibition  $(K_{\text{I}})$  Parameters for PCE, cDCE, and VC Reductive Dechlorination in Cell Suspensions of Geo Strain SZ and Dhc Strain BAV1 in Response to Increasing N<sub>2</sub>O Concentrations<sup>a</sup>

e <sup>-</sup> acceptor	culture	$N_2O(\mu M)$	$V_{ m max}$ (nmol Cl $^-$ min $^{-1}$ mg protein $^{-1}$ )	$K_{ m m} \left( \mu { m M}  ight)$	$K_{ m I} \left( \mu { m M}  ight)$
PCE	strain SZ	0	76.3 (±2.6)	25.1 (±2.9)	40.8 (±3.8)
		10	61.3 (±4.1)		
		60	30.9 (±4.2)		
cDCE	strain BAV1	0	119.4 (±4.1)	19.9 $(\pm 2.5)$	21.2 (±3.5)
		10	81.1 (±5.1)		
		60	31.2 (±2.4)		
VC	strain BAV1	0	123.3 (±3.2)	$18.9 (\pm 1.3)$	$9.6 (\pm 0.4)$
		15	78.9 (±2.1)		
		50	$19.9 (\pm 1.3)$		

<sup>a</sup>The best fit data were achieved with the Michaelis-Menten noncompetitive inhibition model. Error values represent 95% confidence intervals.

values were determined (Figure 4B and 4D; Table 1), indicating that the substrate affinity of the BvcA RDase does not explain the more potent inhibition of the VC-to-ethene dechlorination step by  $N_2O$ .

# DISCUSSION

## Effects of N<sub>2</sub>O on Corrinoid-Dependent Processes.

Toxic effects of  $N_2O$  were first observed in the mid-1950s after two patients died following prolonged  $N_2O$  inhalation.<sup>40</sup> This incident triggered studies to elucidate the mechanism underlying  $N_2O$  toxicity, and detailed investigations revealed that  $N_2O$  reacts with cobalt-containing corrinoids (e.g., cobalamin) when the coordinated cobalt atom is in the reduced Co(I) state. <sup>25,26</sup> Due to the vital roles of enzyme systems with corrinoid prosthetic groups, <sup>30,41</sup> the  $N_2O$ -mediated oxidation of the Co(I) supernucleophile interferes with key metabolic functions in all domains of life. <sup>42,43</sup> For example,  $N_2O$  inhibits the corrinoid-

dependent methionine synthase (MetH) required for the biosynthesis of the essential amino acid methionine. When used as inhalation anesthetic for human patients,  $N_2O$  can lead to a malfunction of MetH, resulting in elevated levels of homocysteine in plasma (i.e., hyperhomocysteinemia). Patients generally recover from  $N_2O$  exposure after 3–4 days, presumably through de novo MetH synthesis or replenishment of Co(I) corrinoid.

The lowest reported  $N_2O$  concentration that affected MetH activity in animals and humans was around 4.1 mM ( $\sim$ 1000 ppm); however, much lower  $N_2O$  concentrations inhibited members of the Bacteria and Archaea, presumably due to the more diverse roles of corrinoid-dependent enzyme systems in their metabolisms. For example, in the denitrifying bacterium Paracoccus denitrificans strain PD1222, 0.1 mM  $N_2O$  not only repressed MetH but also modulated the expression of anabolic genes under the control of vitamin  $B_{12}$  riboswitches. To

compensate for the loss of MetH function, organisms such as P. denitrificans and Escherichia coli activate a corrinoid-independent methionine synthase, MetE.  $^{41,47}$  Geo strain SZ possesses both the metE and the metH genes,  $^{32}$  which may explain the observation that up to 10 mM N<sub>2</sub>O did not inhibit the bacterium's growth with fumarate in defined minimal medium. In contrast, N<sub>2</sub>O at micromolar concentrations inhibited the growth of Geo strain SZ cultures when PCE served as the sole electron acceptor. These observations corroborate that the inhibitory effect of N<sub>2</sub>O to organisms varies markedly based on whether corrinoid-dependent enzyme systems are essential for key metabolic steps, including respiratory energy conservation.

OHRB as a Model To Study the Effects of N<sub>2</sub>O Inhibition. A key feature of OHRB is the involvement of corrinoid-dependent RDases in electron transfer to the chlorinated organohalogen electron acceptor. 1,28,29,48 Functional and structural analyses demonstrated that RDases represent a distinct subfamily of corrinoid-dependent enzymes, and a Co(I) supernucleophile is crucial for RDases to initiate the cleavage of carbon-chlorine bonds. 28,29,49 Since corrinoiddependent RDases are essential in the energy metabolism of OHRB, N<sub>2</sub>O inhibition on Co(I) corrinoid-dependent RDases can be readily observed by quantitative measurement of dechlorination activity and growth when alternate electron acceptors are absent or the energy metabolism of the OHRB is restricted to chlorinated electron acceptors, as is the case for Dhc. This effect was convincingly demonstrated in both Geo strain SZ and Dhc strain BAV1 cultures amended with chlorinated electron acceptors and N2O. Thus, OHRB are excellent model organisms to assess the inhibitory effects of N<sub>2</sub>O on enzymes involving the Co(I) supernucleophile in catalysis. Consistent with this assumption, experimental results showed that N2O at micromolar concentrations exhibited strong inhibitory effects on reductive dechlorination performance in both Geo strain SZ and Dhc strain BAV1 cultures. Theoretically, a shortage of methionine caused by N2O inhibition on MetH could also have affected dechlorination activity; however, growth of Geo strain SZ with fumarate was not impaired at much higher N<sub>2</sub>O concentrations of up to 10 mM, indicating that N<sub>2</sub>O inhibition of RDases diminished dechlorination performance.

The PCE-to-cDCE dechlorinating Geo strain SZ tolerated at least 3-fold higher N2O concentrations than Dhc strain BAV1 before cessation of dechlorination activity was observed, which possibly relates to strain SZ's ability for de novo cobamide biosynthesis.<sup>32</sup> Active cobamide biosynthesis may allow strain SZ to maintain some level of catalytically active PCE RDase. In contrast, the characterized obligate organohalide-respiring Dhc strains<sup>4,50</sup> and *Dehalogenimonas* spp., including the VC-respiring Candidatus Dehalogenimonas etheniformans,<sup>5</sup> cannot de novo synthesize corrinoid, although exceptions may exist.<sup>51</sup> All characterized cDCE and VC dechlorinators strictly require exogenous corrinoid, which renders these bacteria more susceptible to N2O inhibition, and low micromolar concentrations of N<sub>2</sub>O (i.e., 3-10  $\mu$ M) repressed the growth of the corrinoid-auxotroph Dhc strain BAV1. Unlike corrinoidauxotrophic Dehalococcoidia, the majority of PCE-to-TCEand TCE-to-cDCE-dechlorinating OHRB are corrinoid prototrophs,<sup>52</sup> a feature that may enable these organisms to tolerate higher N2O concentrations. The difference in the ability for de novo corrinoid biosynthesis is one possible explanation why PCE and TCE dechlorination to cDCE is generally achieved at sites with nitrate, 16,53 but ethene is not produced.

Corrinoid-dependent enzyme systems fulfill essential metabolic functions for organisms in all branches of life, but only a subset of the bacteria and the archaea have the machinery for de novo corrinoid biosynthesis. Therefore,  $N_2O$  effects on microbial processes that hinge on the activity of corrinoid-dependent enzyme systems may expand beyond organohalide respiration.

Elevated Groundwater N<sub>2</sub>O and Kinetic Parameters. Based the current day atmospheric N<sub>2</sub>O concentration of 330 ppb, the theoretical equilibrium concentration of N<sub>2</sub>O in groundwater should be around 7 nM, assuming no mass transfer limitations; however, much higher groundwater N2O concentrations were reported, indicating other sources exist. 31,56 For example, the increased usage of synthetic nitrogen fertilizer for agricultural production causes substantial nitrate runoff and elevated N<sub>2</sub>O concentrations in groundwater. <sup>19,31</sup> Indeed, correlations between fertilizer application and associated nitrate runoff with elevated groundwater N2O concentrations have been established. 19,56 Nitrate is not conservative, and processes including denitrification, 18,19 respiratory ammonification (i.e., dissimilatory nitrate reduction to ammonium, DNRA)57 ensuing nitrification,<sup>21</sup> as well as chemodenitrification<sup>38</sup> contribute to the formation of N2O. Such biogeochemical processes are likely responsible for elevated N<sub>2</sub>O concentrations, and up to  $140 \,\mu\text{M}\,\text{N}_2\bar{\text{O}}$  was observed in watersheds impacted by agricultural activities. 31 Thus, the N<sub>2</sub>O concentrations measured in many groundwater aquifers exceed the theoretical equilibrium with atmospheric N2O by up to 5 orders in magnitude, and intensified agriculture will exacerbate this issue.

A  $K_{\rm I}$  value indicates the inhibitor (i.e.,  $N_{\rm 2}O$ ) concentration at which the maximum reaction rate  $V_{\rm max}$  (i.e., the reductive dechlorination rates of chlorinated ethenes) is reduced by 50%. The determined  $K_I$  values for  $N_2O$  on reductive dechlorination of PCE, cDCE, and VC are in the range of 40, 20, and 10  $\mu$ M, respectively, well below reported N2O concentrations encountered in many groundwater aquifers, particularly at sites impacted by agricultural runoff.<sup>31</sup> Consequently, N<sub>2</sub>O inhibition could be a major cause for incomplete reductive dechlorination and cDCE and VC stalls observed at field sites. 7-10,53 Of note, a 50%  $V_{\text{max,cDCE}}$  and  $V_{\text{max,VC}}$  inhibition occurred in strain BAV1 at 2- and 4-fold lower N<sub>2</sub>O concentrations, respectively, compared to the same level of inhibition of  $V_{\text{max,PCE}}$  in strain SZ. The higher K<sub>I</sub> values for N<sub>2</sub>O determined for Geo strain SZ compared to strain BAV1 may be related to the ability of strain SZ for de novo corrinoid biosynthesis (see above) or to mechanistic differences in the dechlorination steps catalyzed by the PceA versus the BvcA RDases. Similar K<sub>m</sub> values for cDCE and VC were determined in strain BAV1, indicating the organism exhibits similar affinities for cDCE and VC; however, the 2-fold higher  $K_{\rm I}$ value for the cDCE versus the VC dechlorination step cannot be easily explained considering the same BvcA RDase is involved in both dechlorination steps, \$2,58 and detailed mechanistic studies

Predicting the fate of chlorinated ethenes at bioremediation sites relies on accurate estimates of the intrinsic kinetic parameters of OHRB;  $^{59}$  however, kinetic constants determinations using various dechlorinating cultures at different cell densities reported highly variable  $V_{\rm max}$  and  $K_{\rm m}$  values (or  $K_{\rm S}$  values when Monod kinetics were applied).  $^{12,60,61}$  Likely explanations for these discrepancies are that different, potentially competing types of dechlorinators with distinct RDases and present in varied abundances contributed to reductive dechlorination.  $^{12,62,63}$  The current study accom-

plished kinetic measurements in axenic cultures under defined conditions and over short incubation periods (<6 h, no growth occurred), which facilitates the determination of intrinsic kinetic parameters. The Michaelis—Menten model simulations predicted the behaviors of *Geo* strain SZ and *Dhc* strain BAV1 ( $R^2 > 0.90$ ), and both organisms fit the noncompetitive inhibition model ( $R^2 > 0.96$ ) with micromolar levels of N<sub>2</sub>O as the inhibitor. These findings imply N<sub>2</sub>O as a noncompetitive inhibitor that oxidizes the Co(I) corrinoid cofactor of RDases, thereby decreasing reductive dechlorination rates.

Implications for in Situ Bioremediation. Electron donor (i.e., hydrogen) limitations,6 nutrient availability (e.g., fixed nitrogen), 15 unfavorable redox potential, 7,11 low pH conditions, 14 or toxic and/or inhibitory effects of cocontaminants (e.g., sulfide, chloroform, 1,1,1-trichloroethane) 12,62 can impact the microbial reductive dechlorination process. The findings of the current study indicate that decreased reductive dechlorination performance can be the result of N<sub>2</sub>O inhibition. A common strategy to improve in situ degradation of chlorinated ethenes involves the injection of nutrients (i.e., biostimulation), typically fermentable substrates aimed at increasing the flux of hydrogen.<sup>2,64</sup> The formulations can include fertilizer (nitrate, ammonium, urea, phosphorus) to proactively address possible nutrient limitations. 2,13,15,65 Biogeochemical transformations of fixed nitrogen will generate N<sub>2</sub>O<sup>21,38,57</sup> and exert inhibitory effects on microbial reductive dechlorination, which can result in undesirable cDCE or VC stalls. Thus, practitioners should carefully evaluate the need for fixed nitrogen additions to avoid possible N<sub>2</sub>O inhibition.

The inhibitory constants,  $K_{\rm IP}$  for  $N_{\rm 2}O$  inhibition of PCE, cDCE, and VC dechlorination were within the  $N_{\rm 2}O$  concentration ranges observed in groundwater aquifers (i.e., up to 143  $\mu$ M), <sup>31</sup> suggesting that  $N_{\rm 2}O$  should be of concern at contaminated sites where practitioners seek to rely on microbial reductive dechlorination as a remedial strategy. Considering the relevance of the microbial reductive dechlorination process for achieving cleanup goals and the commonality of elevated  $N_{\rm 2}O$  concentrations in aquifers, groundwater monitoring regimes should include nitrate/nitrite and  $N_{\rm 2}O$  measurements, so that potential inhibition and cDCE and VC stalls can be explained and predicted.

### ASSOCIATED CONTENT

#### S Supporting Information

The Supporting Information is available free of charge on the ACS Publications website at DOI: 10.1021/acs.est.8b05871.

Equations of inhibition models considered in kinetic analyses; raw data of initial dechlorination rates versus corresponding substrate concentrations in cell suspension assays with increasing  $N_2O$  concentrations; inhibition models tested and statistical parameters ( $R^2$ , AICc, and Sy.x values) used for ranking inhibition models; initial versus final amounts of  $N_2O$  determined in growth experiments; competitive and uncompetitive  $N_2O$  inhibition plots of PCE, cDCE, and VC reductive dechlorination (PDF)

#### AUTHOR INFORMATION

### **Corresponding Author**

\*Phone: (865) 974-4933. E-mail: frank.loeffler@utk.edu.

ORCID ®

Frank E. Löffler: 0000-0002-9797-4279

#### **Present Address**

VN.P.: RNA Biology and Molecular Physiology, Faculty of Biology, Bielefeld University, Bielefeld 101133, Germany.

#### Notes

The authors declare no competing financial interest.

#### ACKNOWLEDGMENTS

This work was supported by the Strategic Environmental Research and Development Program (SERDP project ER-2312) and, in part, by awards from the National Institute of Environmental Health Sciences (R01ES024294) and the National Science Foundation (Dimensions DEB1831599). Y.Y participates in the China—University of Tennessee One-Hundred Scholars Program, and the authors acknowledge the support by the China Scholarship Council and the University of Tennessee.

#### REFERENCES

- (1) Adrian, L.; Löffler, F. E. Organohalide-respiring bacteria; Springer: Berlin, Heidelberg, 2016.
- (2) Löffler, F. E.; Edwards, E. A. Harnessing microbial activities for environmental cleanup. *Curr. Opin. Biotechnol.* **2006**, *17* (3), 274–284.
- (3) Sung, Y.; Fletcher, K. E.; Ritalahti, K. M.; Apkarian, R. P.; Ramos-Hernández, N.; Sanford, R. A.; Mesbah, N. M.; Löffler, F. E. *Geobacter lovleyi* sp. nov. strain SZ, a novel metal-reducing and tetrachloroethene-dechlorinating bacterium. *Appl. Environ. Microbiol.* **2006**, 72 (4), 2775–2782.
- (4) Löffler, F. E.; Yan, J.; Ritalahti, K. M.; Adrian, L.; Edwards, E. A.; Konstantinidis, K. T.; Müller, J. A.; Fullerton, H.; Zinder, S. H.; Spormann, A. M. Dehalococcoides mccartyi gen. nov., sp. nov., obligately organohalide-respiring anaerobic bacteria relevant to halogen cycling and bioremediation, belong to a novel bacterial class, Dehalococcoidia classis nov., order Dehalococcoidales ord. nov. and family Dehalococcoidaceae fam. nov., within the phylum Chloroflexi. Int. J. Syst. Evol. Microbiol. 2013, 63 (2), 625–635.
- (5) Yang, Y.; Higgins, S. A.; Yan, J.; Simsir, B.; Chourey, K.; Iyer, R.; Hettich, R. L.; Baldwin, B.; Ogles, D. M.; Löffler, F. E. Grape pomace compost harbors organohalide-respiring Dehalogenimonas species with novel reductive dehalogenase genes. *ISME J.* **2017**, *11* (12), 2767–2780.
- (6) Fennell, D. E.; Gossett, J. M.; Zinder, S. H. Comparison of butyric acid, ethanol, lactic acid, and propionic acid as hydrogen donors for the reductive dechlorination of tetrachloroethene. *Environ. Sci. Technol.* 1997, 31 (3), 918–926.
- (7) Schmidt, K. R.; Tiehm, A. Natural attenuation of chloroethenes: identification of sequential reductive/oxidative biodegradation by microcosm studies. *Water Sci. Technol.* **2008**, *58* (5), 1137–1145.
- (8) Amaral, H. I.; Aeppli, C.; Kipfer, R.; Berg, M. Assessing the transformation of chlorinated ethenes in aquifers with limited potential for natural attenuation: added values of compound-specific carbon isotope analysis and groundwater dating. *Chemosphere* **2011**, 85 (5), 774–781.
- (9) Dugat-Bony, E.; Biderre-Petit, C.; Jaziri, F.; David, M. M.; Denonfoux, J.; Lyon, D. Y.; Richard, J. Y.; Curvers, C.; Boucher, D.; Vogel, T. M.; Peyretaillade, E.; Peyret, P. *In situ* TCE degradation mediated by complex dehalorespiring communities during biostimulation processes. *Microb. Biotechnol.* **2012**, *5* (5), 642–653.
- (10) Tillotson, J. M.; Borden, R. C. Rate and extent of chlorinated ethene removal at 37 ERD sites. *J. Environ. Eng.* **2017**, 143 (8), 04017028.
- (11) Nelson, D. K.; Hozalski, R. M.; Clapp, L. W.; Semmens, M. J.; Novak, P. J. Effect of nitrate and sulfate on dechlorination by a mixed hydrogen-fed culture. *Biorem. J.* **2002**, *6* (3), 225–236.
- (12) Berggren, D. R.; Marshall, I. P.; Azizian, M. F.; Spormann, A. M.; Semprini, L. Effects of sulfate reduction on the bacterial community and kinetic parameters of a dechlorinating culture under chemostat growth conditions. *Environ. Sci. Technol.* **2013**, *47* (4), 1879–1886.

- (13) Steffan, R. J.; Schaefer, C. E. Current and future bioremediation applications: bioremediation from a practical and regulatory perspective. In Organohalide-respiring bacteria; Adrian, L., Löffler, F. E., Eds.; Springer Berlin Heidelberg: Berlin, Heidelberg, 2016; pp 517-540.
- (14) Yang, Y.; Capiro, N. L.; Marcet, T. F.; Yan, J.; Pennell, K. D.; Löffler, F. E. Organohalide respiration with chlorinated ethenes under low pH conditions. Environ. Sci. Technol. 2017, 51 (15), 8579-8588.
- (15) Lendvay, J. M.; Löffler, F. E.; Dollhopf, M.; Aiello, M. R.; Daniels, G.; Fathepure, B. Z.; Gebhard, M.; Heine, R.; Helton, R.; Shi, J. Bioreactive barriers: a comparison of bioaugmentation and biostimulation for chlorinated solvent remediation. Environ. Sci. Technol. 2003, 37 (7), 1422-1431.
- (16) Lee, J.; Im, J.; Kim, U.; Löffler, F. E. A data mining approach to predict In situ detoxification potential of chlorinated ethenes. Environ. Sci. Technol. 2016, 50 (10), 5181-5188.
- (17) He, J.; Sung, Y.; Krajmalnik-Brown, R.; Ritalahti, K. M.; Löffler, F. E. Isolation and characterization of Dehalococcoides sp. strain FL2, a trichloroethene (TCE)-and 1,2-dichloroethene-respiring anaerobe. Environ. Microbiol. 2005, 7 (9), 1442-1450.
- (18) Zumft, W. G. Cell biology and molecular basis of denitrification. Microbiol Mol. Biol. Rev. 1997, 61 (4), 533-616.
- (19) Thomson, A. J.; Giannopoulos, G.; Pretty, J.; Baggs, E. M.; Richardson, D. J. Biological sources and sinks of nitrous oxide and strategies to mitigate emissions. Philos. Trans. R. Soc., B 2012, 367 (1593), 1157-1168.
- (20) Zhu, X.; Burger, M.; Doane, T. A.; Horwath, W. R. Ammonia oxidation pathways and nitrifier denitrification are significant sources of N<sub>2</sub>O and NO under low oxygen availability. Proc. Natl. Acad. Sci. U. S. A. 2013, 110 (16), 6328-6333.
- (21) Daims, H.; Lücker, S.; Wagner, M. A new perspective on microbes formerly known as nitrite-oxidizing bacteria. Trends Microbiol. **2016**, 24 (9), 699–712.
- (22) Balderston, W. L.; Payne, W. J. Inhibition of methanogenesis in salt marsh sediments and whole-cell suspensions of methanogenic bacteria by nitrogen oxides. Appl. Environ. Microbiol. 1976, 32 (2), 264-269.
- (23) Klüber, H. D.; Conrad, R. Inhibitory effects of nitrate, nitrite, NO and N2O on methanogenesis by methanosarcina barkeri and Methanobacterium bryantii. FEMS Microbiol. Ecol. 1998, 25, 331-339.
- (24) Tugtas, A. E.; Pavlostathis, S. G. Inhibitory effects of nitrogen oxides on a mixed methanogenic culture. Biotechnol. Bioeng. 2007, 96 (3), 444-455.
- (25) Banks, R. G. S.; Henderson, R. J.; Pratt, J. M. Reactions of gases in solution. Part III. Some reactions of nitrous oxide with transition-metal complexes. J. Chem. Soc. A 1968, No. 0, 2886-2889.
- (26) Blackburn, R.; Kyaw, M.; Swallow, A. J. Reaction of cob(I)alamin with nitrous oxide and cob(III)alamin. J. Chem. Soc., Faraday Trans. 1 **1977**, 73 (0), 250–255.
- (27) Fischer, R.; Thauer, R. K. Methanogenesis from acetate in cell extracts of Methanosarcina barkeri: isotope exchange between CO2 and the carbonyl group of acetyl-CoA, and the role of H<sub>2</sub>. Arch. Microbiol. **1990**, 153 (2), 156–162.
- (28) Bommer, M.; Kunze, C.; Fesseler, J.; Schubert, T.; Diekert, G.; Dobbek, H. Structural basis for organohalide respiration. Science 2014, 346 (6208), 455-458.
- (29) Payne, K. A.; Quezada, C. P.; Fisher, K.; Dunstan, M. S.; Collins, F. A.; Sjuts, H.; Levy, C.; Hay, S.; Rigby, S. E.; Leys, D. Reductive dehalogenase structure suggests a mechanism for B<sub>12</sub>-dependent dehalogenation. Nature 2015, 517 (7535), 513-516.
- (30) Yan, J.; Bi, M.; Bourdon, A. K.; Farmer, A. T.; Wang, P. H.; Molenda, O.; Quaile, A. T.; Jiang, N.; Yang, Y.; Yin, Y.; Şimşir, B.; Campagna, S. R.; Edwards, E. A.; Löffler, F. E. Purinyl-cobamide is a native prosthetic group of reductive dehalogenases. Nat. Chem. Biol. **2017**, 14 (1), 8–14.
- (31) Jurado, A.; Borges, A. V.; Brouyere, S. Dynamics and emissions of N<sub>2</sub>O in groundwater: A review. Sci. Total Environ. 2017, 584-585, 207-

- (32) Wagner, D. D.; Hug, L. A.; Hatt, J. K.; Spitzmiller, M. R.; Padilla-Crespo, E.; Ritalahti, K. M.; Edwards, E. A.; Konstantinidis, K. T.; Löffler, F. E. Genomic determinants of organohalide-respiration in Geobacter lovleyi, an unusual member of the Geobacteraceae. BMC Genomics 2012, 13 (1), 200.
- (33) He, J.; Ritalahti, K. M.; Yang, K. L.; Koenigsberg, S. S.; Löffler, F. E. Detoxification of vinyl chloride to ethene coupled to growth of an anaerobic bacterium. Nature 2003, 424 (6944), 62-65.
- (34) Yan, J.; Şimşir, B.; Farmer, A. T.; Bi, M.; Yang, Y.; Campagna, S. R.; Löffler, F. E. The corrinoid cofactor of reductive dehalogenases affects dechlorination rates and extents in organohalide-respiring Dehalococcoides mccartyi. ISME J. 2016, 10 (5), 1092-1101.
- (35) Wolin, E. A.; Wolin, M. J.; Wolfe, R. S. Formation of methane by bacterial extracts. J. Biol. Chem. 1963, 238 (8), 2882-2886.
- (36) Sander, R. Compilation of Henry's law constants (version 4.0) for water as solvent. Atmos. Chem. Phys. 2015, 15 (8), 4399-4981.
- (37) Bradford, M. M. A rapid and sensitive method for the quantitation of microgram quantities of protein utilizing the principle of protein-dye binding. Anal. Biochem. 1976, 72 (1), 248-254.
- (38) Onley, J. R.; Ahsan, S.; Sanford, R. A.; Löffler, F. E. Denitrification by Anaeromyxobacter dehalogenans, a common soil bacterium lacking the nitrite reductase genes nirS and nirK. Appl. Environ. Microbiol. 2018, 84 (4), e01985-17.
- (39) Iverson, T. M.; Luna-Chavez, C.; Cecchini, G.; Rees, D. C. Structure of the *Escherichia coli* fumarate reductase respiratory complex. Science 1999, 284 (5422), 1961-1966.
- (40) Lassen, H. C. A.; Henriksen, E.; Neukirch, F.; Kristensen, H. Treatment of tetanus. Severe bone-marrow depression after prolonged nitrous-oxide anaesthesia. Lancet 1956, 267, 527-530.
- (41) Matthews, R. G. Cobalamin- and corrinoid-dependent enzymes. Met Ions Life Sci. 2009, 6, 53-114.
- (42) Drummond, J. T.; Matthews, R. G. Nitrous oxide degradation by cobalamin-dependent methionine synthase: characterization of the reactants and products in the inactivation reaction. Biochemistry 1994, 33, 3732-3741.
- (43) Drummond, J. T.; Matthews, R. G. Nitrous oxide inactivation of cobalamin-dependent methionine synthase from Escherichia coli: characterization of the damage to the enzyme and prosthetic group. Biochemistry 1994, 33 (12), 3742-3750.
- (44) Royston, B. D.; Nunn, J. F.; Weinbren, H. K.; Royston, D.; Cormack, R. S. Rate of inactivation of human and rodent hepatic methionine synthase by nitrous oxide. Anesthesiology 1988, 68 (2),
- (45) Singer, M. A.; Lazaridis, C.; Nations, S. P.; Wolfe, G. I. Reversible nitrous oxide-induced myeloneuropathy with pernicious anemia: case report and literature review. Muscle Nerve 2008, 37 (1), 125-129.
- (46) Weimann, J. Toxicity of nitrous oxide. Bailliere's Best Pract. Res., Clin. Anaesthesiol. 2003, 17 (1), 47-61.
- (47) Sullivan, M. J.; Gates, A. J.; Appia-Ayme, C.; Rowley, G.; Richardson, D. J. Copper control of bacterial nitrous oxide emission and its impact on vitamin  $\mathrm{B}_{12}$ -dependent metabolism. *Proc. Natl. Acad.* Sci. U. S. A. 2013, 110 (49), 19926-19931.
- (48) Wang, S.; Qiu, L.; Liu, X.; Xu, G.; Siegert, M.; Lu, Q.; Juneau, P.; Yu, L.; Liang, D.; He, Z.; Qiu, R. Electron transport chains in organohalide-respiring bacteria and bioremediation implications. Biotechnol. Adv. 2018, 36 (4), 1194-1206.
- (49) Fincker, M.; Spormann, A. M. Biochemistry of catabolic reductive dehalogenation. Annu. Rev. Biochem. 2017, 86, 357-386.
- (50) Seshadri, R.; Adrian, L.; Fouts, D. E.; Eisen, J. A.; Phillippy, A. M.; Methe, B. A.; Ward, N. L.; Nelson, W. C.; Deboy, R. T.; Khouri, H. M.; Kolonay, J. F.; Dodson, R. J.; Daugherty, S. C.; Brinkac, L. M.; Sullivan, S. A.; Madupu, R.; Nelson, K. E.; Kang, K. H.; Impraim, M.; Tran, K.; Robinson, J. M.; Forberger, H. A.; Fraser, C. M.; Zinder, S. H.; Heidelberg, J. F. Genome sequence of the PCE-dechlorinating bacterium Dehalococcoides ethenogenes. Science 2005, 307 (5706), 105-108.
- (51) Brisson, V. L.; West, K. A.; Lee, P. K. H.; Tringe, S. G.; Brodie, E. L.; Alvarez-Cohen, L. Metagenomic analysis of a stable trichloroethenedegrading microbial community. ISME J. 2012, 6 (9), 1702-1714.

- (52) Schubert, T.; Adrian, L.; Sawers, R. G.; Diekert, G. Organohalide respiratory chains: composition, topology and key enzymes. *FEMS Microbiol Ecol* **2018**, 94 (4), fiy035.
- (53) Verce, M. F.; Madrid, V. M.; Gregory, S. D.; Demir, Z.; Singleton, M. J.; Salazar, E. P.; Jackson, P. J.; Halden, R. U.; Verce, A. A long-term field study of *in situ* bioremediation in a fractured conglomerate trichloroethene source zone. *Biorem. J.* **2015**, *19* (1), 18–31.
- (54) Shelton, A. N.; Seth, E. C.; Mok, K. C.; Han, A. W.; Jackson, S. N.; Haft, D. R.; Taga, M. E. Uneven distribution of cobamide biosynthesis and dependence in bacteria predicted by comparative genomics. *ISME J.* **2018**, DOI: 10.1038/s41396-018-0304-9.
- (55) Zhang, Y.; Rodionov, D. A.; Gelfand, M. S.; Gladyshev, V. N. Comparative genomic analyses of nickel, cobalt and vitamin  $B_{12}$  utilization. *BMC Genomics* **2009**, *10* (1), 78.
- (56) Reay, D. S.; Davidson, E. A.; Smith, K. A.; Smith, P.; Melillo, J. M.; Dentener, F.; Crutzen, P. J. Global agriculture and nitrous oxide emissions. *Nat. Clim. Change* **2012**, *2* (6), 410–416.
- (57) Yoon, S.; Cruz-García, C.; Sanford, R.; Ritalahti, K. M.; Löffler, F. E. Denitrification versus respiratory ammonification: environmental controls of two competing dissimilatory NO<sub>3</sub><sup>-</sup>/NO<sub>2</sub><sup>-</sup> reduction pathways in *Shewanella loihica* strain PV-4. *ISME J.* **2015**, *9* (5), 1093–1104.
- (58) Tang, S.; Chan, W. W. M.; Fletcher, K. E.; Seifert, J.; Liang, X.; Löffler, F. E.; Edwards, E. A.; Adrian, L. Functional characterization of reductive dehalogenases by using blue native polyacrylamide gel electrophoresis. *Appl. Environ. Microbiol.* **2013**, *79* (3), 974–981.
- (59) Huang, D.; Becker, J. G. Determination of intrinsic monod kinetic parameters for two heterotrophic tetrachloroethene (PCE)-respiring strains and insight into their application. *Biotechnol. Bioeng.* **2009**, *104* (2), 301–311.
- (60) Baelum, J.; Scheutz, C.; Chambon, J. C.; Jensen, C. M.; Brochmann, R. P.; Dennis, P.; Laier, T.; Broholm, M. M.; Bjerg, P. L.; Binning, P. J.; Jacobsen, C. S. The impact of bioaugmentation on dechlorination kinetics and on microbial dechlorinating communities in subsurface clay till. *Environ. Pollut.* **2014**, *186*, 149–157.
- (61) Mayer-Blackwell, K.; Fincker, M.; Molenda, O.; Callahan, B.; Sewell, H.; Holmes, S.; Edwards, E. A.; Spormann, A. M. 1,2-dichloroethane exposure alters the population structure, metabolism, and kinetics of a trichloroethene-dechlorinating *Dehalococcoides mccartyi* consortium. *Environ. Sci. Technol.* **2016**, *50* (22), 12187–12196.
- (62) Chan, W. W.; Grostern, A.; Löffler, F. E.; Edwards, E. A. Quantifying the effects of 1,1,1-trichloroethane and 1,1-dichloroethane on chlorinated ethene reductive dehalogenases. *Environ. Sci. Technol.* **2011**, 45 (22), 9693–9702.
- (63) Buttet, G. F.; Murray, A. M.; Goris, T.; Burion, M.; Jin, B.; Rolle, M.; Holliger, C.; Maillard, J. Coexistence of two distinct *Sulfurospirillum* populations respiring tetrachloroethene genomic and kinetic considerations. *FEMS Microbiol Ecol* **2018**, *94* (5), fiy018.
- (64) McCarty, P. L. Groundwater contamination by chlorinated solvents: History, remediation technologies and strategies. In *In Situ remediation of chlorinated solvent plumes*; Stroo, H. F., Ward, C. H., Eds.; Springer New York: New York, 2010; pp 1–28.
- (65) Schaefer, C. E.; Lippincott, D. R.; Steffan, R. J. Field-scale evaluation of bioaugmentation dosage for treating chlorinated ethenes. *Groundwater Monit. Rem.* **2010**, *30* (3), 113–124.